

Supporting Information

Single-Nanowire-on-Film as an Efficient SERS-Active Platform

Il-sun Yoon,[†] Taejoon Kang,[†] Wonjun Choi,[‡] Jangbae Kim,^{†,&} Youngdong Yoo,[†] Sang-Woo Joo,[§]

Q-Han Park,[‡] Hyotcherl Ihee,^{*,†,&} and Bongsoo Kim^{*,†}

[†]Department of Chemistry, KAIST, Daejeon 305-701, Korea,

[‡]Department of Physics, Korea University, Seoul 136-701, Korea,

[&]Center for Time-Resolved Diffraction, KAIST, Daejeon 305-701, Korea,

[§]Department of Chemistry, Soongsil University, Seoul 156-743, Korea.

Characterization of a Au NW synthesized by the vapor transport method.

Figure S1(a) shows a scanning electron microscope (SEM) image of as-synthesized Au NWs on a sapphire substrate. NWs are tens of μm long and have diameters of 100 ~ 200 nm. The inset is a high-magnification SEM image of a Au NW tip, showing that the NW has a unique diamond shaped cross section and an angled tip. The high resolution transmission electron microscope (HRTEM) image and the selected area electron diffraction pattern (SAED) in Figure S1(b) show that the NW has a nearly atomistically flat surface and clear single crystallinity. The lattice spacing of 0.144 nm, consistent with the (110) crystal plane of the face centered cubic (*fcc*) Au, confirms that the NW grew in the preferred direction of [110]. The high crystallinity and purity of the Au NW are supported by an X-ray diffraction (XRD) pattern and energy-dispersive X-ray spectrometry (EDS) analyses (Figures S2 and S3). The XRD pattern of as-grown NWs is successfully indexed to the *fcc* structure of Au with a lattice parameter $a = 0.4072$ nm of a space group *Fm*3m (225). The EDS spectrum shows that the NW contains only Au.

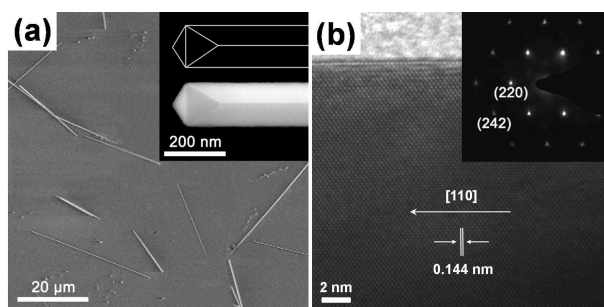


Figure S1. (a) SEM image of Au NWs on a sapphire substrate. The inset is a high-magnification SEM image of a single Au NW showing an angled tip and a diamond shaped cross section. (b) HRTEM image of a Au NW. Atomistically flat surface is clearly observed. The inset is an SAED pattern of the NW.

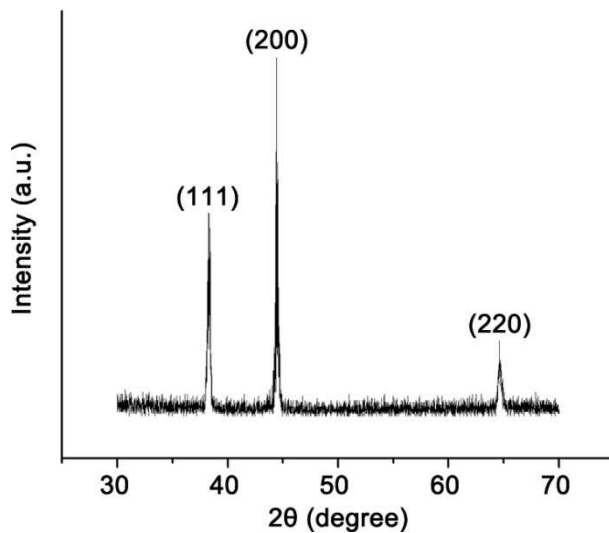


Figure S2. XRD pattern of as-grown Au NWs was recorded using a Rigaku D/max-RC (12 kW) diffractometer with the Cu K α radiation ($\lambda = 1.5406 \text{ \AA}$). Three distinguished peaks are indexed perfectly to the *fcc* phase of Au (Fm3m, $a = 0.4072 \text{ nm}$). This pattern is very close to the reported data (JPCDS File no. 65-8601).

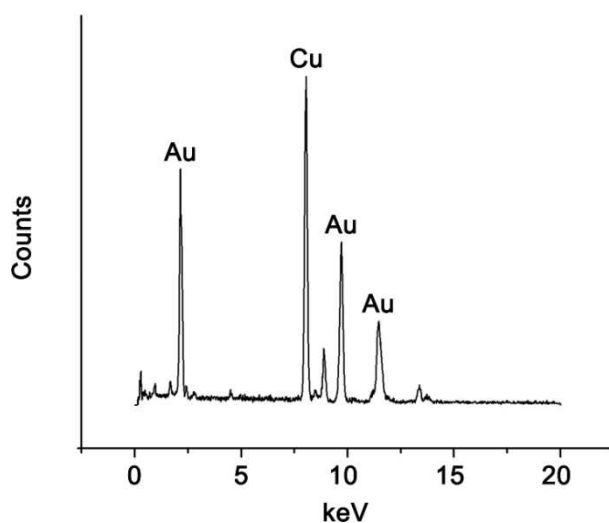


Figure S3. Chemical composition of the NW was studied by the TEM-EDS analysis. Only Au peaks are seen except some peaks from copper which are due to the TEM grid. This confirms that the NW contains only Au.

AFM images of smooth Au and Ag films

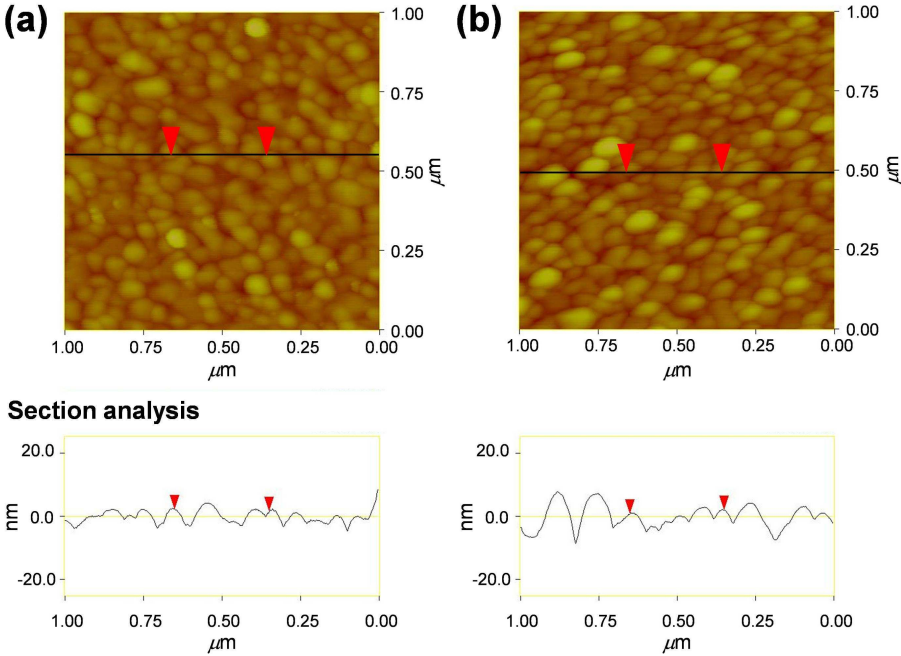


Figure S4. AFM images of smooth (a) Au and (b) Ag films prepared by e-beam assisted deposition of 10-nm Cr, followed by 300-nm Au or Ag on precleaned silicon substrates. The AFM images were recorded by a Nanoscope IIIa (Digital Instruments). The root-mean-square-roughness of (a) Au and (b) Ag films were 2.3 and 2.8 nm, respectively, as measured by an AFM.

FDTD studies of a Au NW on a Au film (Au/Au SNOF) and a Au NW on a Si substrate.

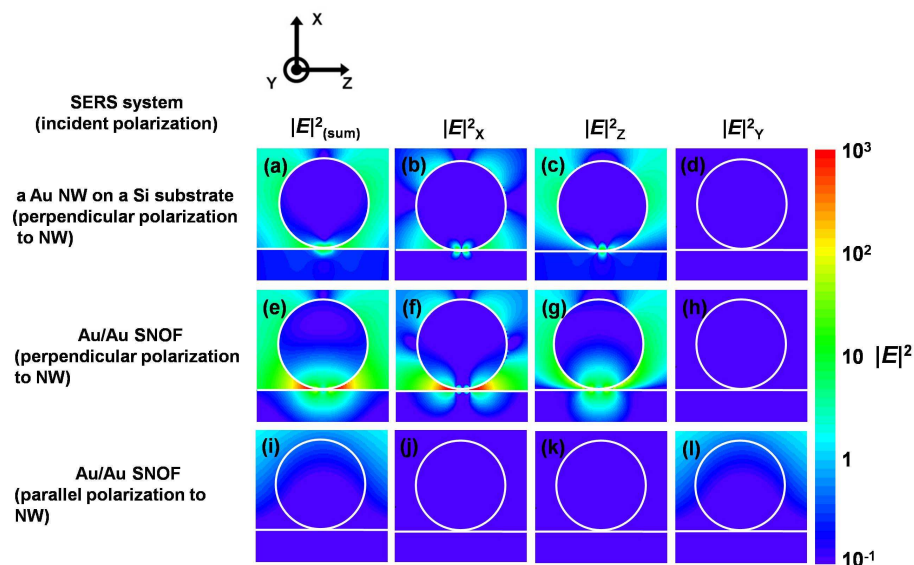


Figure S5. X, Y, and Z components of the electric field and their summation around a Au NW on a Si substrate system and Au/Au SNOF predicted by FDTD calculations: (a-d) single NW on a Si substrate with a perpendicular polarization, (e-h) Au/Au SNOF with a perpendicular polarization, and (i-l) Au/Au SNOF with a parallel polarization. The 632.8 nm light is incident on the NW along the $-X$ direction with perpendicular (Z -axis directed) or parallel (Y -axis directed) polarization direction to the NW.

SERS enhancement of Au/Au SNOF with respect to a smooth Au film.

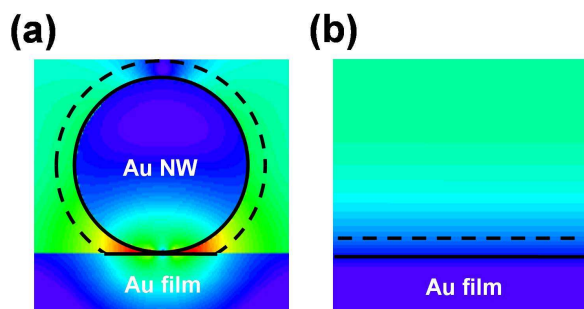


Figure S6. The squared electric field intensities, $|E|^4$, are integrated to evaluate the SERS enhancements in the following volumes of Au/Au SNOF and a smooth Au film. a) When the SNOF is excited by perpendicularly polarized light, strongly enhanced electric field is induced at the gap between the NW

and the film. The volume within 10 nm from the surface of the NW and along the NW axis with a 500 nm length was set as the SERS-active region of SNOF and integrated. b) The volume within the cylinder of a 500 nm diameter and a 10 nm height on the surface of the Au film was integrated for a smooth Au film.

Additional FDTD studies for understanding SERS enhancement of SNOF.

To further understand SERS enhancement of SNOF, we calculated how the electric field enhancement of Au/Au SNOF changed as a function of the diameter of the Au NW, the thickness of the Au film, the gap distance between the Au NW and the Au film, and the angle of the incident light referenced to the Au film plane. Figure S7 shows that the SERS enhancement of Au/Au SNOF is dependent on the diameter of the Au NW and maximized when the diameter of the NW is ~ 80 nm. Figure S8 shows that SERS enhancement is determined by the thickness of the film and the gap distance between the NW and the film. The SERS enhancement gets higher as the gap distance decreases and the film becomes thicker. The SERS enhancement is maximized when the NW directly contacts the film and the thickness of the film is larger than 100 nm. In this case, the film acts like a perfect mirror and does not allow the incident and the Raman scattered lights to penetrate the film. Figure S9 shows that the distribution of the electric field of SNOF changes as the angle of the incident light is varied. The SERS enhancement of SNOF decreases as the incident angle changes from normal to parallel to the film and the electric field of the illuminated side of the NW is partially enhanced at the gap of the NW and the film.

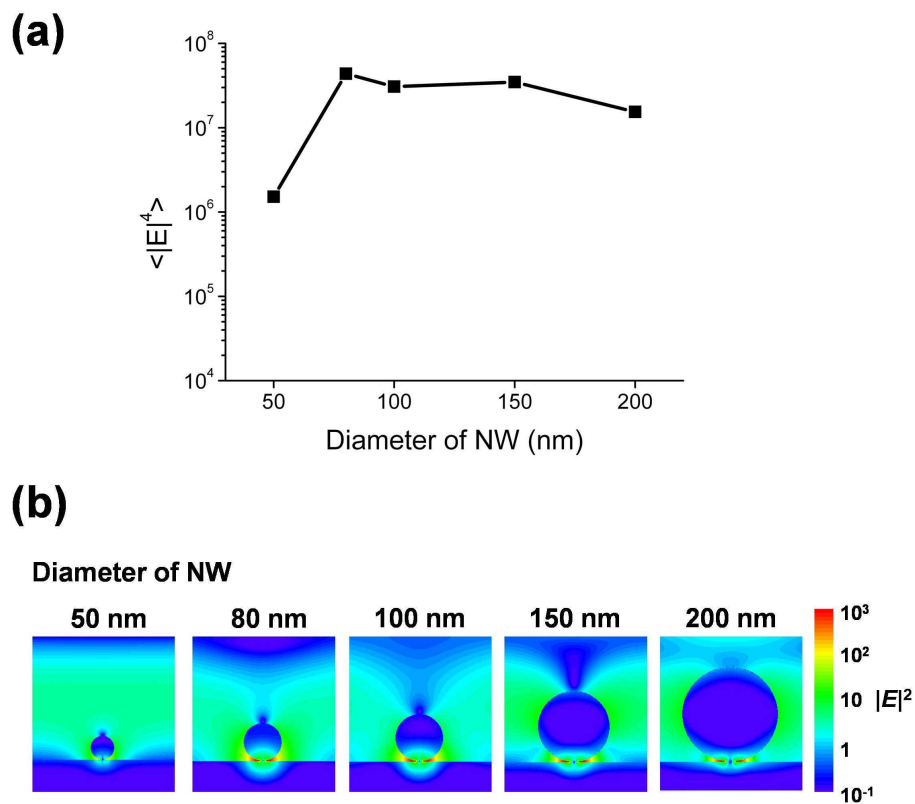


Figure S7. (a) The graph shows the dependence of the integrated value of the squared electric field intensity on the diameter of the NW. (b) The dependence of the electric field intensity of Au/Au SNOF on the diameter of the NW.

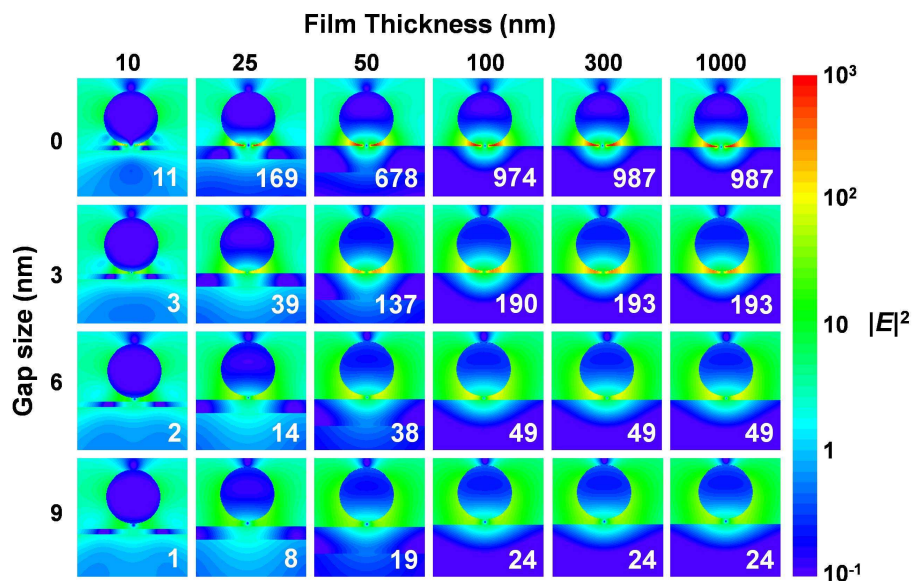


Figure S8. The dependence of the electric field intensity of the Au/Au SNOF on the thickness of the

film and the gap distance between a NW and a film. Data with combinations of six selected thicknesses (10, 25, 50, 100, 300, and 1000 nm as indicated at the top) and four selected gap sizes (0, 3, 6, and 9 nm as indicated at the left) comprise 24 cases. The numbers in the lower right corner of each image indicate the integrated value of the squared electric field intensity divided by the lowest value obtained when the gap distance is 9 nm and the thickness is 10 nm.

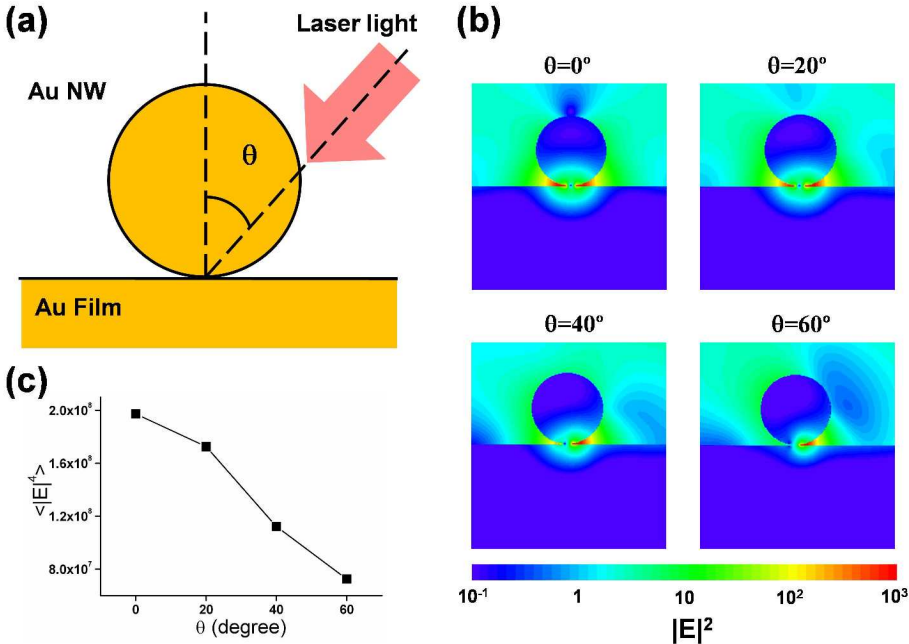


Figure S9. (a) Schematic illustration of the Au/Au SNOF with variation of the angle of the incident light. θ is defined as an angle of the incident light direction relative to the normal axis of the film plane. (b) The dependence of the electric field intensities of SNOF on θ . (c) The dependence of the integrated value of the squared electric field intensity on θ .